LEARNING GRAPH REPRESENTATIONS FOR INFLUENCE MAXIMIZATION

Anonymous authors
Paper under double-blind review

ABSTRACT

As the field of machine learning for combinatorial optimization advances, traditional problems are resurfaced and readdressed through this new perspective. The overwhelming majority of the literature focuses on small graph problems, while several real-world problems are devoted to large graphs. Here, we focus on two such problems: influence estimation, a #P-hard counting problem, and influence maximization, an NP-hard problem. We develop GLIE, a Graph Neural Network (GNN) that inherently parameterizes an upper bound of influence estimation and train it on small simulated graphs. Experiments show that GLIE provides accurate influence estimation for real graphs up to 10 times larger than the train set. More importantly, it can be used for influence maximization on considerably larger graphs, as the predictions ranking is not effected by the drop of accuracy. We develop a version of Cost Effective Lazy Forward optimization with GLIE instead of simulated influence estimation, surpassing the benchmark for influence maximization, although with a computational overhead. To balance the time complexity and quality of influence, we propose two different approaches. The first is a Q-network that learns to choose seeds sequentially using GLIE's predictions. The second defines a provably submodular function based on GLIE's representations to rank nodes fast while building the seed set. The latter provides the best combination of time efficiency and influence spread, outperforming SOTA benchmarks.

1 INTRODUCTION

Several real-world problems can be cast as a combinatorial optimization problem over a graph. From distributing packages Mathew et al. (2015) to improving the general health Wilder et al. (2018) and vehicles' management Touati-Moungla & Jost (2012), optimization on graphs lies in the core of many real-world applications that are vital to our way of living. Unfortunately, the majority of these problems are NP-hard, and hence we can only approximate their solution in a satisfactory time limit that matches the real world requirements. Recent machine learning methods have emerged as a promising solution to develop heuristic methods that provide fast and accurate approximations Bengio et al. (2020). The general idea is to train a supervised or unsupervised learning model to infer the solution given an unseen graph and the problem constraints. The models tend to consist of Graph Neural Networks (GNNs) to encode the graph and the nodes, Q-learning Watkins & Dayan (1992); Sutton & Barto (2018) to produce sequential predictions, or a combination of both. The practical motivation behind learning to solve combinatorial optimization problems, is that inference time is faster than running an exact combinatorial solver Joshi et al. (2019). That said, specialized combinatorial algorithms like CONCORDE for the *Traveling Salesman Problem* (TSP) or GUROBI in general, cannot be surpassed yet Kool et al. (2018).

Though many such methods have been proposed for a plethora of problems, influence maximization (IM) has not been addressed yet extensively. IM addresses the problem of finding the set of nodes in a network that would maximize the number of nodes reached by starting a diffusion from them Kempe et al. (2003). The problem is proved to be NP-hard, from a reduction to the set-cover problem. Moreover, the influence estimation (IE) problem that is embedded in IM, i.e., estimating the number of nodes influenced by a given seed set, is #P-hard as it is analogous to counting s-t connectedness and would require $2^{|E|}$ possible combinations to compute exactly, where $|E|$ is the number of network

edges Wang et al. (2012). Typically, influence estimation is approximated using repetitive Monte-Carlo (MC) simulations of the independent cascade (IC) diffusion model. In general, the seed set is built greedily, taking advantage of the submodularity of the influence function which guarantees an at least $(1 - \frac{1}{e})$ approximation to the optimal. Although the latter lacks of efficiency as one still has to estimate influence for every candidate seed in every step of building the seed sets. Hence, several scalable algorithms Borgs et al. (2014); Tang et al. (2015) and heuristics Chen et al. (2009); Jung et al. (2012) were developed capitalizing on sketches or the structure of the graph to produce more efficient solutions. IM can be applied on a plethora of real-world tasks, such as epidemic containment Wilder et al. (2017), diminishing fake news Budak et al. (2011), and running viral marketing campaigns Domingos & Richardson (2001).

We address IM through the perspective of deep learning for combinatorial optimization. More specifically, we propose GLIE, a GNN that provides efficient IE for a given seed set and a graph with influence probabilities. It can be used as a standalone influence predictor with competitive results for graphs up to 10 times larger than the train set. Moreover, we leverage GLIE for IM, combining it with CELF Leskovec et al. (2007), that typically does not scale beyond networks with thousands of edges. The proposed method runs in networks with millions of edges in seconds, and exhibits better influence spread than a state-of-the-art algorithm and previous GNN-RL methods for IM. In addition, we develop GRIM a Q-learning architecture that utilizes GLIE's representations and predictions to obtain seeds sequentially, while minimizing the number of influence estimations throughout steps. Finally, we propose a heuristic based on GLIE's representations that represents the number of neighbors predicted to be uninfluenced and acts as an approximation to the marginal gain, PUN. We prove that it is submodular and hence can be optimized greedily. The experiments indicate PUN provides the best balance between influence quality and computational efficiency.

The paper is organized as follows. Section 2 presents an overview of relevant approaches and clarifies the advantage of the our models. Section 3 describes the four proposed methods, starting with IE and advancing progressively towards faster methods for IM. Section 4 exhibits and interprets the experimental results for IE and IM. Finally Section 5 summarizes the contribution and presents future steps.

2 RELATED WORK

The first approach to solving combinatorial optimization (CO) using neural networks was based on attention-based NNs for discrete structures, POINTERNETS Vinyals et al. (2015), followed by an architecture that combines POINTERNETS with an actor-critic training to find the best route for TSP Bello et al. (2016). The first architecture that utilized graph-based learning was S2N-DQN Dai et al. (2017), which used STRUCT2VEC to encode the states of the nodes and the graph, and uses them to train a Q-learning model Sutton & Barto (2018) that chooses the right node to add in a solution given the current state.

Based on S2V-DQN, a DQN Mnih et al. (2015) for the network dismantling problem was recently proposed Fan et al. (2020). The model, named FINDER, uses a deep Q-learning architecture along with three GRAPHSAGE layers. The reward is based on size of the giant connected component size, i.e., every new node (seed) chosen, aims to dismantle the network as much as possible. The main advantage of FINDER is that it is trained on small synthetic data while it can extrapolate to relatively large graphs. On the other hand, one of its core disadvantages is that it can not work with directed graphs and weighted edges. Moreover it addresses a proxy problem Morone & Makse (2015) rather than traditional IM. Another recent supervised deep learning approach on IM, GCOMB Manchanda et al. (2020), leverages a probabilistic greedy method to produce scores on graphs of the training set and uses them to teach a GNN to predict such scores. A Q-network receives the score along with the maximum score from all nodes as graph state, and an approximate calculation of the seed's neighborhood correlation with the seed set, to predict the Q-value of a node. Though very scalable and comparable to state-of-the-art in influence, GCOMB has to be trained on a large random subset of the test graph. This means the model has to be retrained for every new test graph, which imposes a serious overhead considering the time required for producing the scores using MC ICs and training. To be specific, it needs to be trained on 30% of the graph and tested on the rest, a preprocessing that in practice takes hours, as noted in the supplementary material G Manchanda et al. (2020). Hence GCOMB is optimized for scalability but not for time efficiency, and is not comparable to the current

works which run in seconds. We note here that the majority of the relevant literature on DL for CO address very small graphs Vinyals et al. (2015); Kool et al. (2018); Prates et al. (2019) which renders them as well not applicable to our task. More scalable, unsupervised methods Karalias & Loukas (2020) are tailored to specific problems and is non-trivial to adjust them to our problem.

The current work combines the advantages of the aforementioned methods, in that it is only trained on small simulated data once and generalizes to larger graphs, while it addresses the problem of IM in weighted directed networks. The main idea is separating IE and IM, and train a supervised model for IE. Afterwards, we have the freedom to use the trained model to develop various approaches, ranging from a new version of a classical algorithm, a Q-learning approach that resembles the recent literature, and a fast submodular function to rank nodes based on the model's representations.

3 METHODOLOGY

3.1 GRAPH LEARNING FOR INFLUENCE ESTIMATION (GLIE)

In this section, we introduce GLIE (**G**NN **L**earning **I**nfluence **E**stimation), which aims to learn how to estimate the influence of a seed set S over a graph $G = (V, E)$. Let $\mathbf{A} \in \mathbb{R}^{n \times n}$ be the adjacency matrix and $\mathbf{X} \in \mathbb{R}^{n \times d}$ be the features of nodes, representing which nodes belong to the seed set by 1 and 0 otherwise:

$$\mathbf{X}_u = \begin{cases} \{1\}^d, & u \in S \\ \{0\}^d, & u \notin S \end{cases} . \tag{1}$$

For the derivation of the corollary, we set $d = 1$. More dimensions will become meaningful when we parameterize the problem. If we normalize $\mathbf{A}$ by each row, we form a row-stochastic transition matrix, as:

$$\mathbf{A}_{uv} = p_{vu} = \begin{cases} \frac{1}{\deg(u)}, & v \in \mathcal{N}(u) \\ 0, & v \notin \mathcal{N}(u) \end{cases} , \tag{2}$$

where $\deg(u)$ is the in-degree of node u and $\mathcal{N}(u)$ is the set of neighbors of u. Based on the weighted cascade Kempe et al. (2003), each row u stores the probability of node u being influenced by each of the other nodes that are connected to it by a directed link $v \to u$. Note that, in case of directed influence graphs, $\mathbf{A}$ should correspond to the *transpose* of the adjacency matrix. The influence probability $p(u|S)$ resembles the probability of a node u getting influenced if its neighbors belong in the seed set, i.e., during the first step of the diffusion. We can use message passing to compute a well-known upper bound $\hat{p}(u|S)$ of $p(u|S)$ for node u:

$$\hat{p}(u|S) = \mathbf{A}_u \cdot \mathbf{X} = \sum_{v \in \mathcal{N}(u) \cap S} \frac{1}{\deg(u)} = \sum_{v \in \mathcal{N}(u) \cap S} p_{vu} \geq 1 - \prod_{v \in \mathcal{N}(u) \cap S} (1 - p_{vu}) = p(u|S), \tag{3}$$

where the second equality stems from the definition of the weighted cascade and the inequality from the proof in Zhou et al. (2015) App. A. As the diffusion covers more than one-hop, the derivation requires repeating the multiplication to approximate the total influence spread. To be specific, computing the influence probability of nodes that are not adjacent to the seed set requires estimating recursively the probability of their neighbors being influenced by the seeds. If we let $\mathbf{H}_1 = \mathbf{A} \cdot \mathbf{X}$, and we assume the new seed set S^t to be the nodes influenced in the step $t - 1$, their probabilities are stored in $\mathbf{H}_t$, much like a diffusion in discrete time. We can then recompute the new influence probabilities with $\mathbf{H}_{t+1} = \mathbf{A} \cdot \mathbf{H}_t$,

Corollary 3.0.1. *The repeated product $\mathbf{H}_{t+1} = \mathbf{A} \cdot \mathbf{H}_t$ computes an upper bound to the real influence probabilities of each infected node at step $t + 1$.*

The proof can be found in Appendix A.2. In reality, due to the existence of cycles, two problems arise with this computation. Firstly, if the process is repeated the influence of the original seeds may increase again, which comes in contrast with the independent cascade model. This can be controlled by minimizing the repetitions, e.g., four repetitions cause the original seeds to be able to reinfect other nodes in a network with triangles. To this end, we leverage up to three neural network layers. Another problem due to cycles pertains to the probability of neighbors influencing each other. In this case, the product of the complementary probabilities in Eq. (3) does not factorize for the non-independent neighbors. This effect was analyzed extensively in Lokhov & Saad (2019) App. B and proved that the

influence probability computed by $p(u|S)$ is itself an upper bound on the real influence probability for graphs with cycles. Intuitively, the product that represents non-independent probabilities is larger than the product of independent ones. This renders the real influence probability, which is complementary to the product, smaller than what we compute.

We can thus contend that the estimation $\hat{p}(u|S)$ provides an upper bound on the real influence probability—and we can use it to compute an upper bound to the real influence spread of a given seed set i.e., the total number of nodes influenced by the diffusion. Since message passing can compute inherently an approximation of influence estimation, we can parameterize it to learn a function that tightens this approximation based on supervision. In our neural network architecture, each layer consists of a GNN with a batchnorm and dropout omitted here, and starting from $\mathbf{H}_0 = \mathbf{X} \in \mathbb{R}^{n \times d}$ we have:

$$\mathbf{H}_{t+1} = \text{ReLU}([\mathbf{H}_t, \mathbf{A}\mathbf{H}_t]\mathbf{W}_0). \tag{4}$$

The readout function that summarizes the graph representation based on all nodes' representations is a summation over all the final representations with skip connections:

$$\mathbf{H}_S^G = \sum_{v \in V} [\mathbf{H}_0^v, \mathbf{H}_1^v, \ldots, \mathbf{H}_t^v]. \tag{5}$$

This representation captures the probability of all nodes being active throughout each layer. The output that represents the predicted influence spread is derived by:

$$\hat{\sigma}(S) = \text{ReLU}(\mathbf{H}_S^G \mathbf{W}_o). \tag{6}$$

3.2 Cost Effective Lazy Forward with GLIE (CELF-GLIE)

The original Cost Effective Lazy Forward Leskovec et al. (2007) is an acceleration to the original greedy algorithm that is based on the constraint that a seed's spread will never get bigger in subsequent steps. The influence spread is computed for every node in the first iteration and kept in a sorted list. In each step, the marginal gain is computed for the node with the best influence spread in the previous round. If it is better than the previously second node, it is chosen as the next seed because it is necessarily bigger than the rest. This property stems from submodularity, i.e., the marginal gain can never increase with the size of the seed set. If the first node's current gain is smaller than the second previous gain, the list is resorted and the process is repeated until the best node is found. The worst-case complexity is similar to greedy but in practice it can be hundreds of times faster, while retaining greedy's original guarantee of $(1 - 1/e)$.

In our case, we propose a straight forward adaptation where we substitute the original CELF IE based on MC IC with the output of GLIE. We redirect the reader in the Appendix B, where we show that the estimations of GLIE are monotonous and submodular in practice, and hence $\hat{\sigma}$ is suitable for optimizing with CELF. CELF-GLIE has two main computational bottlenecks. First, although it alleviates the need to test every node in every step, in practice it still requires IE for more than one nodes in each step. Second, it requires computing the initial IE for every node in the first step. We will try to alleviate both with the two subsequent methods.

3.3 Graph Reinforcement Learning for Influence Mazimization (GRIM)

We develop a method that computes only one IE in every step, along with the initial IE for all nodes. We first define the influence set representation $L_S \in \{0, 1\}^n$, which can be computed by adding the activations of each layer $\mathbf{H}_t$, summing along the axis of the hidden layer size, and thresholding to get a binary vector:

$$L_S = \mathbb{1}\left\{\sum_{t=0}^{T} \frac{\sum_{i=0}^{d_t} \mathbf{H}_t^i}{d_t} \geq 0\right\}, \tag{7}$$

where T is the number of layers, and $\mathbf{H}_t^i \in \mathbb{R}^{n \times 1}$ is a column from $\mathbf{H}_t$. This vector contains a label for each node whose sign indicates if it is predicted to be influenced. We utilize this to compute the difference between the influence of the current seed set and the initial influence of each other node.

We aim to build a method that learns how to pick seeds sequentially. The model needs to receive information from GLIE regarding the state (graph and seed set), and decide on the next action

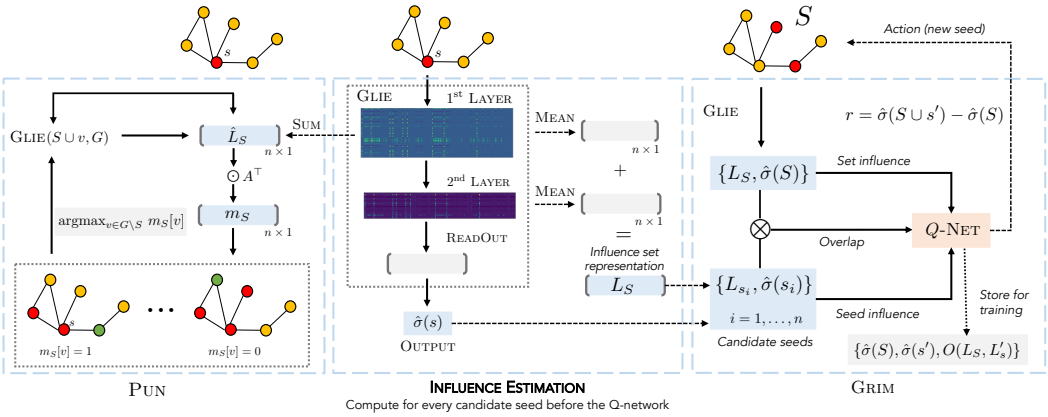

Figure 1: A visual depiction of the pipeline for GRIM and PUN. The layers of GLIE are depicted by a heatmap of an actual seed during inference time, showing how the values vary through different nodes (columns).

(seed). Note that, GLIE can not provide a direct estimate of a new candidate's s marginal gain without rerunning GLIE$(S \cup s, G)$, which is what we try to avoid. To this end, we utilize a double Q-network Van Hasselt et al. (2016) and the model is depicted in Fig. 1 (middle and right part). During the first step, GLIE provides an IE for all candidate seeds, and the node with the highest is added to the seed set, similar to GLIE-CELF. We also keep a list of each node's initial influence set L_s. Subsequently, the Q-network produces a Q-value for each node s using as input the estimated influence of the current seed set $\hat{\sigma}(S)$, the initial influence of the node $\hat{\sigma}(s)$, and the interaction between them. The interaction is defined as the difference between their corresponding influence sets $O(S, s) = \sum_{i=0}^{n} \mathbb{1}\{L_s^i - L_S^i \geq 0\}$, as predicted by GLIE. The latter aims to measure how different is the candidate node from the seed set, in order to quantify the potential gain of adding it. The Q-network is called **G**raph **R**einforcement for **I**nfluence **M**aximization (GRIM), and its architecture is composed by two layers:

$$Q(u, S, G) = \text{ReLU}(\text{ReLU}([\hat{\sigma}_S, \hat{\sigma}_s, O(S, s)]\mathbf{W}_k)\mathbf{W}_q), \tag{8}$$

where $\mathbf{W}_q \in \mathbb{R}^{hd \times 1}$, and hd is the hidden layer size. We utilize a greedy policy to choose the next seed, similar to Dai et al. (2017): $\pi(u|S) = \arg\max_{u \in S} Q(u, S, G)$. Given the chosen action u, the reward is computed based on the marginal gain, i.e., the estimated influence of the new seed set minus the influence of the seed set before the action, as computed by GLIE in:

$$r = \hat{\sigma}(S \cup u) - \hat{\sigma}(S). \tag{9}$$

During training, we use epsilon-greedy to simulate an IM "game" and balance between exploration and exploitation. We store as a train tuple the current state-action embedding $\{\hat{\sigma}(S), \hat{\sigma}(s'), O(S, s')\}$, the new state embedding along with all next possible actions $\{\hat{\sigma}(S \cup s), \hat{\sigma}(s), O(S, s)\}, s \in V$ and the reward r. Throughout the IM, we randomly sample from the memory and train the parameters of GRIM. GLIE is frozen, because apart from providing graph and node embeddings, it is only used for the computation of the reward—thus, it is not updated. The strategy to pretrain a graph encoding layer on a supervised task and use it as part of the Q-network has proven beneficial in similar works Mirhoseini et al. (2021). In our case though we found out that without the overlap O and with simpler features such as the degree, the model performs rather poorly, which means we can not alleviate the burden of computing IE for every node in the first step.

3.4 POTENTIALLY UNINFLUENCED NEIGHBORS (PUN)

Computing the influence spread of every (or even some selected) nodes in the first step is very computationally demanding, as we will also empirically examine in the experiments section. We thus seek a method that can surpass this hinder and provide adequate performance. We first need to redefine a simpler influence set representation based on GLIE's representations. Let $\hat{L}_S \in \{0, 1\}^n$ be

the binary vector with 1s in nodes predicted to be uninfluenced and 0s elsewhere:

$$\hat{L}_S = \mathbb{1}\left\{\sum_{i=0}^{d_1} \mathbf{H}_1^i \leq 0\right\}. \tag{10}$$

$\hat{L}_S$ is obviously simpler than L_S defined in Eq. (7), and provides a more rough estimate, but we need this definition to prove that our function is submodular and optimize it greedily. Using these, we can use message passing to predict the amount of a node's neighborhood that remains uninfluenced, i.e., the **P**otentially **U**ninfluenced **N**eighbors (PUN), weighted by the respective probability of influence:

$$m_S = A^\top \cdot \hat{L}_S \in \mathbb{R}^{n\times 1}. \tag{11}$$

Maximizing this heuristic can be considered an approximation to a seed's marginal gain on its immediate neighbors. In accordance to the definition of the marginal gain, the influence spread is the summation of the marginal gains of every incremental seed set i, up to S:

$$\sigma^m(S) = \sum_{i=1}^{|S|} m_{S_i}. \tag{12}$$

In order to establish that σ^m can be optimized greedily with a theoretical guarantee of $(1-\frac{1}{e})$OPT, we need to prove its monotonocity and submodularity. The monotonicty is straight forward as it is a cumulative quantity of a non negative measure m.

Theorem 1. *The influence spread σ^m is submodular.*

The proof can be found in the Appendix A.2. PUN can be seen in the left part of Fig. 1. We start by setting the first seed as the node with the highest degree, which can be considered a safe assumption as in practice it is always part of seed sets. We use GLIE(S, G) to retrieve $\hat{L}_S$, which we use to find the next node based on $\arg\max_{v\in G\setminus S} m_S[v]$ and the new $\hat{L}_{S\cup\{v\}}$. One disadvantage of PUN is that σ^m is an underestimation of the predicted influence, as can be seen in Fig. 2. Contrasted with the upper bound, DMP, σ^m is not as accurate as $\hat{\sigma}$, but allows us to compute efficiently a submodular proxy for the marginal gain. This underestimation means that a part of the network considered uninfluenced in $\hat{L}_S$ is measured as potential gain for their neighbors, hence the ranking based on m_S can be effected negatively. As we observed in Fig. 2, the divergence of σ^m increases with the size of the seed set.

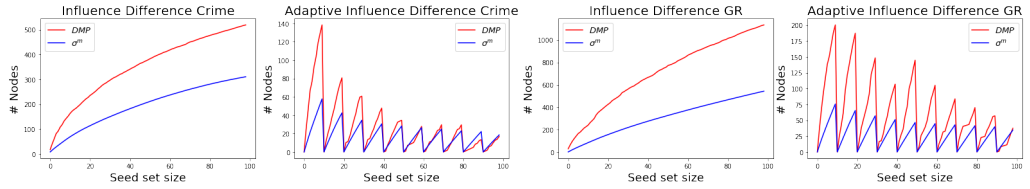

(a) (b) (c) (d)

Figure 2: Difference between DMP influence estimate and σ^m in standard IM and adaptive IM with full feedback every 10 seeds, in two datasets (Crime and GR).

For this purpose, we will use adaptive full-feedback selection (AFF), where after selecting a new seed node, we remove it from the network along with nodes predicted to be influenced. It has been proved in the seminal work of Golovin & Krause (2011) that an AFF greedy algorithm for a submodular and monotonic function is guaranteed to have a competitive performance with the optimal policy. In our case, we will use an AFF update every k seeds, as it adds a small computational overhead if we do it in every step. The benefit to PUN is twofold. Firstly, as we remove the influenced node and truncate the seed set, GLIE produces a more valid estimate because it performs better when the graph and seed set are smaller. Secondly, as the neighborhood size decreases, the effect of missed influenced nodes is diminished in m_S. These can be observed in the "Adaptive" plots of Fig. 2 (b), (d) and in other related figures in Appendix B, where we employ an AFF every 10 seeds and we contrast the aforementioned gap between the upper bound DMP and $\sigma^m(S)$.

	Graph	# Nodes	# Edges
Sim	Test/Train	$100-500$	$950-4,810$
	Large	$1,000-2,000$	$11,066-19,076$
Small	Crime (CR)	829	$2,946$
	HI-II-14 (HI)	$4,165$	$26,172$
	GR Colab (GR)	$5,242$	$28,980$
Large	Enron (EN)	$33,697$	$361,622$
	Facebook (FB)	$63,393$	$1,633,660$
	Youtube (YT)	$1,134,891$	$5,975,246$

Table 1: Graph datasets.

4 EXPERIMENTS

All the experiments are performed in a PC with an NVIDIA GPU TITAN V (12GB RAM), 256GB RAM and an Intel(R) Xeon(R) W-2145 CPU @ 3.70GHz. The python implementation can be found in the supplementary material.

4.1 INFLUENCE ESTIMATION

For training in the influence estimation task, we create a set of labeled samples, each consisting of the seed set S and the corresponding influence spread $\sigma(S)$. We create 100 Barabasi-Albert Barabási & Albert (1999) and Holme-Kim Holme & Kim (2002) undirected graphs ranging from 100 to 200 nodes and 30 from 300 to 500 nodes. 60% are used for training, 20% for validation and 20% for testing. We have used these network models because the degree distribution resembles the one of real world networks. The influence probabilities are assigned based on the weighted cascade model, i.e., a node u has equal probability $1/\text{deg}(u)$ to be influenced by each of her $\mathcal{N}(u)$ nodes. This model requires a directed graph, hence we turn all undirected graphs to directed ones by appending reverse edges. Though estimating influence probabilities is a problem on its own Panagopoulos et al. (2020), in the absence of extra data, the weighted cascade is considered more realistic than pure random assignments Kempe et al. (2003). To label the samples, we run the CELF algorithm using $1,000$ Monte Carlo (MC) ICs for influence estimation, for up to 5 seeds. The optimum seed set for size 1 to 5 is stored, along with 30 random negative samples for each seed set size. Each sample is accompanied with its ground truth influence spread computed with MC ICs. This amounts to a total of $20,150$ training samples. The rest of the training parameters are described in 5.

We evaluate the models in three different types of graphs. The first is the test set of the dataset mentioned above. The second is a set of 10 power-law large graphs ($1,000$ – $2,000$ nodes) to evaluate the capability of the model to generalize in networks that are larger by one factor. The third is a set of three real-world graphs, namely the *Crime* (CR), *HI-II-14* (HI), and *GR collaborations* (GR). More information about the datasets is given in Table 1. The real graphs are evaluated for varying seed set sizes, from 2 to 10, to test our model's capacity to extrapolate to larger seed set sizes. Due to the size of the latter two graphs (HI and GR), we take for each seed set size the top nodes based on the degree as the optimum seed set along with a 30 random seed sets for the large simulated graphs and 3 for the real graphs, to validate the accuracy of the model in non-significant sets of nodes.

We have compared the accuracy of influence estimation with DMP Lokhov & Saad (2019). We could not utilize the influence estimation of UBLF Zhou et al. (2015) because its central condition is violated by the weighted cascade model and the computed influence is exaggerated to the point it surpasses the nodes of the network. The average error throughout all datasets and the average influence can be seen in Table 2, along with the average time.We evaluate the retrieved seed set using the independent cascade, and the results are shown in Table 3. We should underline here that this task would require more then 3 hours for the *Crime* dataset and days for *GR* using the traditional approach with $1,000$ MC IC. As we can see in Table 3, GLIE-CELF allows for a significant acceleration in computational time, while the retrieved seeds are more effective. Moreover, in CELF, the majority of time is consumed in the initial computation of the influence spread, i.e., the overhead to compute 100 instead of the 20 seeds shown in Table 3, amounts to 0.11, 0.22 and 0.19 seconds for the three datasets respectively.

Graph (seeds)	**AVG Influence**	DMP		GLIE	
		MAE	**Time (Sec)**	**MAE**	**Time (Sec)**
Test set (1 – 5)	17.01	1.30	0.05	0.79	0.0042
Large set (1 – 5)	78.52	6.78	0.44	8.07	0.0034
CR (1 – 10)	59.71	0.59	0.11	2.65	0.0029
HI (1 – 10)	297.23	12.38	2.84	17.72	0.0034
GR (1 – 10)	39.60	4.85	4.32	3.34	0.0042

Table 2: Average mean absolute error (MAE) and time (seconds) throughout all seed set sizes and samples, along with the real average influence spread.

Graph (20 **seeds**)	**Seed Overlap**	DMP-CELF		GLIE-CELF	
		Influence	**Time (Sec)**	**Influence**	**Time (Sec)**
CR	14	221	83	229	1.0
HI	13	$1,235$	$8,362$	$1,281$	5.49
GR	12	295	$16,533$	393	7.01

Table 3: Influence maximization for **20** seeds with CELF, using the proposed (GLIE) substitute for influence estimation and evaluating with $1,000$ MC independent cascades (IC).

4.2 INFLUENCE MAXIMIZATION

GRIM is trained on a dataset that consists of 50 random BA graphs of $500 - 2,000$ nodes. It is trained by choosing 100 seeds sequentially, to maximize the reward (delay = 2 steps) for each network. Since the immediate reward corresponds to the marginal gain, the sum of these rewards at the end of the "game" corresponds to the total influence of the seed set. An episode corresponds to completing the game for all 50 graphs; we play 500 episodes, taking roughly 40 seconds each. The exploration is set to 0.3 and declines with a factor of 0.99. The model is optimized using ADAM, as in GLIE. We store the model that has the best average influence over all train graphs in a training episode. In order to diminish the computational time of the first step in GLIE-CELF and GRIM, we focus on candidate seeds that surpass a certain degree threshold based on the distribution, a common practice in the literature Chen et al. (2009); Manchanda et al. (2020) .

For comparison, we use a state-of-the-art IM method, IMM Tang et al. (2015) which capitalizes on reverse reachable sets Borgs et al. (2014) to estimate influence. Specifically, it produces a series of such influence sketches and uses them to approximate the influence spread without any simulation when building the seed set. This results in remarkable acceleration while retaining a theoretical guarantee with high probability. Note that, IMM is considered state-of-the-art and has similar influence spreads with Tang et al. (2014), while surpassing various heuristics Jung et al. (2012). We set $e = 0.5$ as proposed by the authors. We also compare with FINDER, which is analyzed in Section 2.

	20 **seeds**					100 **seeds**				
Graph	PUN	GRIM	GLIE-CELF	IMM	FINDER	PUN	GRIM	GLIE-CELF	IMM	FINDER
CR	<u>229</u>	**232**	228	228	**232**	<u>520</u>	510	**522**	516	502
GR	376	208	**402**	<u>387</u>	379	$1,079$	993	$\mathbf{1,102}$	<u>$1,085$</u>	897
HI	$\mathbf{1,316}$	$1,304$	$1,300$	$\mathbf{1,316}$	$1,110$	$\mathbf{2,313}$	$2,282$	<u>$2,307$</u>	$2,282$	$2,274$
EN	$\mathbf{8,208}$	$8,185$	$8,189$	$\mathbf{8,208}$	$3,964$	$\mathbf{14,920}$	$\mathbf{14,920}$	$\mathbf{14,920}$	$14,848$	$12,596$
FB	$4,280$	<u>$4,480$</u>	$\mathbf{4,487}$	$4,463$	$1,823$	$8,409$	$7,418$	$\mathbf{8,710}$	<u>$8,625$</u>	$5,746$
YT	$104,129$	$104,824$	<u>$105,658$</u>	$\mathbf{105,888}$	$3,799$	$190,656$	$189,515$	$\mathbf{194,834}$	<u>$194,521$</u>	$34,941$

Table 4: Influence spread computed by MC ICs for 20 and 100 seeds.

The results for the influence spread of 20 and 100 seeds as computed by simulations of MC ICs can be seen in Table 4, while the time results for 100 seeds are shown in Table 5. One can see that GLIE-CELF exhibits overall superior influence quality compared to the rest of the methods, but is quite slower. GRIM is slightly faster than GLIE-CELF but is the second slowest method. This quantifies the substantial overhead caused by computing the influence spread of all candidate seeds in

Graph	PUN	GRIM	GLIE-CELF	IMM	FINDER
CR	0.15	0.91	1.25	**0.13**	0.41
GR	**0.17**	0.69	3.41	0.57	2.36
HI	**0.17**	2.59	1.20	0.56	1.01
EN	**0.52**	4.85	5.89	4.78	9.3
FB	**1.42**	100	120.6	69.9	56.8
YT	**13.2**	48	119	55.4	191

Table 5: Computational time in seconds for retrieving 100 seeds.

the first step. Their time difference amounts to how many more IEs GLIE-CELF performs in every step compared to GRIM, which performs only one. This is more obvious with PUN, which requires only one IE in every step and no initial computation. It is from 3 to 60 times faster than IMM while its computational overhead moving from smaller to larger graphs is less than linear to the number of nodes. In terms of influence quality, PUN is first or second in half of the datasets in both seed set sizes. We can thus contend that it provides the best accuracy-efficiency tradeoff from the examined methods. IMM is the third slowest method, but it is very accurate, specially for smaller seed set sizes. FINDER exhibits the least accurate performance, which is understandable given that it solves a relevant problem and not exactly IM for IC. The computational time presented is the time required to solve the node percolation, in which case it may retrieve a bigger seed set than 100 nodes. Thus, we can hypothesize it is quite faster for a limited seed set, but the quality of the retrieved seeds is the least accurate among all methods.

5 CONCLUSION

We have proposed GLIE, a GNN-based solution for the problem of influence estimation. We showcase its accuracy in the respective task and utilized it to address more effectively the problem of influence maximization. We developed three methods based on the representations and the predictions of GLIE. GLIE-CELF, an adaptation of a classical algorithm that surpasses SOTA but with significant computational overhead. GRIM, a Q-learning model that learns to retrieve seeds sequentially using GLIE's predictions and representations. And PUN, a submodular function that acts as proxy for the marginal gain and can be optimized adaptively, striking a balance between efficiency and accuracy.

Influence maximization in the real world could be benefited by supplementary information regarding the properties of the network. A typical IM algorithm needs a significant contribution in order to take into account the topic of the information shared or the user's characteristics Chen et al. (2016) i.e., conditional diffusion. An important practical advantage of a neural network approach is the easy incorporation of such complementary data by adding the corresponding embeddings in the input, as has been done in similar settings Tian et al. (2020). We thus deem an experiment with contextual information a natural next step, given a proper dataset. Our approach can also be utilized to address the minimum vertex cover in large graphs, as it is a problem related to influence maximization and there exists models that work well in both Manchanda et al. (2020). Finally, we also plan to examine the potential of training online the reinforcement learning, i.e., receiving real feedback from each step of the diffusion that could update both, the Q-NET and GLIE. This would allow the model to adjust its decisions based on the partial feedback received during the diffusion.

Ethics and Reproducibility Our influence maximization methods can potentially be used for large scale manipulation in social media. For example, targeting the right susceptible users with specific political advertisements might maximize the effect of the campaign on the general intent to vote. On the bright side, there has been extensive research on battling such effects Tu et al. (2020), by producing campaigns that are equally effective and hence balancing each other Bharathi et al. (2007). More importantly, GLIE can be used as part of the mitigation strategy Tu et al. (2020), as a black box that substitutes the method's RR-set based influence estimation, to actually increase the balance of political exposure in the given social network for the running campaigns. Moreover, our methods can inherently be utilized in the context of limiting fake news spreading similar to other influence maximization algorithms Budak et al. (2011).

Regarding the reproducibility of our experiments, we have attached all codes in the supplementary files along with detailed instructions on how to reproduce the results. We also point to the codes we utilized to run the benchmarks. All data can be downloaded through an anonymous repository.

REFERENCES

Albert-László Barabási and Réka Albert. Emergence of scaling in random networks. *science*, 286 (5439):509–512, 1999.

Irwan Bello, Hieu Pham, Quoc V Le, Mohammad Norouzi, and Samy Bengio. Neural combinatorial optimization with reinforcement learning. *arXiv preprint arXiv:1611.09940*, 2016.

Yoshua Bengio, Andrea Lodi, and Antoine Prouvost. Machine learning for combinatorial optimization: a methodological tour d'horizon. *European Journal of Operational Research*, 2020.

Shishir Bharathi, David Kempe, and Mahyar Salek. Competitive influence maximization in social networks. In *International workshop on web and internet economics*, pp. 306–311. Springer, 2007.

Christian Borgs, Michael Brautbar, Jennifer Chayes, and Brendan Lucier. Maximizing social influence in nearly optimal time. In *Proceedings of the twenty-fifth annual ACM-SIAM symposium on Discrete algorithms*, pp. 946–957. SIAM, 2014.

Stephen Boyd, Stephen P Boyd, and Lieven Vandenberghe. *Convex optimization*. Cambridge university press, 2004.

Ceren Budak, Divyakant Agrawal, and Amr El Abbadi. Limiting the spread of misinformation in social networks. In *Proceedings of the 20th international conference on World wide web*, pp. 665–674, 2011.

Wei Chen, Yajun Wang, and Siyu Yang. Efficient influence maximization in social networks. In *Proceedings of the 15th ACM SIGKDD international conference on Knowledge discovery and data mining*, pp. 199–208, 2009.

Wei Chen, Tian Lin, and Cheng Yang. Real-time topic-aware influence maximization using preprocessing. *Computational social networks*, 3(1):1–19, 2016.

Hanjun Dai, Elias B Khalil, Yuyu Zhang, Bistra Dilkina, and Le Song. Learning combinatorial optimization algorithms over graphs. *arXiv preprint arXiv:1704.01665*, 2017.

Pedro Domingos and Matt Richardson. Mining the network value of customers. In *Proceedings of the seventh ACM SIGKDD international conference on Knowledge discovery and data mining*, pp. 57–66, 2001.

Changjun Fan, Li Zeng, Yizhou Sun, and Yang-Yu Liu. Finding key players in complex networks through deep reinforcement learning. *Nature Machine Intelligence*, pp. 1–8, 2020.

Daniel Golovin and Andreas Krause. Adaptive submodularity: Theory and applications in active learning and stochastic optimization. *Journal of Artificial Intelligence Research*, 42:427–486, 2011.

Petter Holme and Beom Jun Kim. Growing scale-free networks with tunable clustering. *Physical review E*, 65(2):026107, 2002.

Gareth James, Daniela Witten, Trevor Hastie, and Robert Tibshirani. *An introduction to statistical learning*, volume 112. Springer, 2013.

Chaitanya K Joshi, Thomas Laurent, and Xavier Bresson. On learning paradigms for the travelling salesman problem. *arXiv preprint arXiv:1910.07210*, 2019.

Kyomin Jung, Wooram Heo, and Wei Chen. Irie: Scalable and robust influence maximization in social networks. In *2012 IEEE 12th International Conference on Data Mining*, pp. 918–923. IEEE, 2012.

Nikolaos Karalias and Andreas Loukas. Erdos goes neural: an unsupervised learning framework for combinatorial optimization on graphs. *arXiv preprint arXiv:2006.10643*, 2020.

David Kempe, Jon Kleinberg, and Éva Tardos. Maximizing the spread of influence through a social network. In *Proceedings of the ninth ACM SIGKDD international conference on Knowledge discovery and data mining*, pp. 137–146, 2003.

Wouter Kool, Herke Van Hoof, and Max Welling. Attention, learn to solve routing problems! *arXiv preprint arXiv:1803.08475*, 2018.

Jure Leskovec, Andreas Krause, Carlos Guestrin, Christos Faloutsos, Jeanne VanBriesen, and Natalie Glance. Cost-effective outbreak detection in networks. In *Proceedings of the 13th ACM SIGKDD international conference on Knowledge discovery and data mining*, pp. 420–429, 2007.

Andrey Y Lokhov and David Saad. Scalable influence estimation without sampling. *arXiv preprint arXiv:1912.12749*, 2019.

Sahil Manchanda, Akash Mittal, Anuj Dhawan, Sourav Medya, Sayan Ranu, and Ambuj Singh. Gcomb: Learning budget-constrained combinatorial algorithms over billion-sized graphs. *Advances in Neural Information Processing Systems*, 33, 2020.

Neil Mathew, Stephen L Smith, and Steven L Waslander. Planning paths for package delivery in heterogeneous multirobot teams. *IEEE Transactions on Automation Science and Engineering*, 12 (4):1298–1308, 2015.

Azalia Mirhoseini, Anna Goldie, Mustafa Yazgan, Joe Wenjie Jiang, Ebrahim Songhori, Shen Wang, Young-Joon Lee, Eric Johnson, Omkar Pathak, Azade Nazi, et al. A graph placement methodology for fast chip design. *Nature*, 594(7862):207–212, 2021.

Volodymyr Mnih, Koray Kavukcuoglu, David Silver, Andrei A Rusu, Joel Veness, Marc G Bellemare, Alex Graves, Martin Riedmiller, Andreas K Fidjeland, Georg Ostrovski, et al. Human-level control through deep reinforcement learning. *nature*, 518(7540):529–533, 2015.

Flaviano Morone and Hernán A Makse. Influence maximization in complex networks through optimal percolation. *Nature*, 524(7563):65–68, 2015.

George Panagopoulos, Fragkiskos Malliaros, and Michalis Vazirgiannis. Multi-task learning for influence estimation and maximization. *IEEE Transactions on Knowledge and Data Engineering*, 2020.

Marcelo Prates, Pedro HC Avelar, Henrique Lemos, Luis C Lamb, and Moshe Y Vardi. Learning to solve np-complete problems: A graph neural network for decision tsp. In *Proceedings of the AAAI Conference on Artificial Intelligence*, volume 33, pp. 4731–4738, 2019.

Richard S Sutton and Andrew G Barto. *Reinforcement learning: An introduction*. MIT press, 2018.

Youze Tang, Xiaokui Xiao, and Yanchen Shi. Influence maximization: Near-optimal time complexity meets practical efficiency. In *Proceedings of the 2014 ACM SIGMOD international conference on Management of data*, pp. 75–86, 2014.

Youze Tang, Yanchen Shi, and Xiaokui Xiao. Influence maximization in near-linear time: A martingale approach. In *Proceedings of the 2015 ACM SIGMOD International Conference on Management of Data*, pp. 1539–1554, 2015.

Shan Tian, Songsong Mo, Liwei Wang, and Zhiyong Peng. Deep reinforcement learning-based approach to tackle topic-aware influence maximization. *Data Science and Engineering*, 5(1):1–11, 2020.

Nora Touati-Moungla and Vincent Jost. Combinatorial optimization for electric vehicles management. *Journal of Energy and Power Engineering*, 6(5):738–743, 2012.

Sijing Tu, Cigdem Aslay, and Aristides Gionis. Co-exposure maximization in online social networks. *Advances in Neural Information Processing Systems*, 33, 2020.

Hado Van Hasselt, Arthur Guez, and David Silver. Deep reinforcement learning with double q-learning. In *Proceedings of the AAAI Conference on Artificial Intelligence*, volume 30, 2016.

Oriol Vinyals, Meire Fortunato, and Navdeep Jaitly. Pointer networks. *arXiv preprint arXiv:1506.03134*, 2015.

Chi Wang, Wei Chen, and Yajun Wang. Scalable influence maximization for independent cascade model in large-scale social networks. *Data Mining and Knowledge Discovery*, 25(3):545–576, 2012.

Christopher J. C. H. Watkins and Peter Dayan. Q-learning. In *Machine Learning*, pp. 279–292, 1992.

Bryan Wilder, Amulya Yadav, Nicole Immorlica, Eric Rice, and Milind Tambe. Uncharted but not uninfluenced: Influence maximization with an uncertain network. In *AAMAS*, volume 17, pp. 1305–1313, 2017.

Bryan Wilder, Han-Ching Ou, Kayla de la Haye, and Milind Tambe. Optimizing network structure for preventative health. In *AAMAS*, pp. 841–849, 2018.

Chuan Zhou, Peng Zhang, Wenyu Zang, and Li Guo. On the upper bounds of spread for greedy algorithms in social network influence maximization. *IEEE Transactions on Knowledge and Data Engineering*, 27(10):2770–2783, 2015.

SUPPLEMENTARY MATERIAL: LEARNING GRAPH REPRESENTATIONS FOR INFLUENCE MAXIMIZATION

Section 5 gathers the proofs of theorems and corollaries. Section 5 includes plots in support of the arguements in the main text.

APPENDIX A

We recall the first corollary from Sec. 3 and detail the proof below.

Corollary 3.0.2. *The repeated product* $\mathbf{H}_{t+1} = \mathbf{A} \cdot \mathbf{H}_t$ *computes an upper bound to the real influence probabilities of each infected node at step* $t+1$.

Proof. We have:

$$\begin{aligned}
\hat{p}^t(u|S^t) &= \mathbf{A}_u \cdot \mathbf{H}_t && (13)\\
&= \sum_{v \in \mathcal{N}(u) \cap S^t} \hat{p}_v p_{vu} && (14)\\
&\geq \sum_{v \in \mathcal{N}(u) \cap S^t} p_v p_{vu} && (15)\\
&\geq 1 - \prod_{v \in \mathcal{N}(u) \cap S^t} (1 - p_v p_{vu}) && (16)\\
&= p^t(u|S^t) && (17)\\
& && (18)
\end{aligned}$$

- (15) stems from Eq. 3 in the manuscript:

$$\hat{p}(u|S) = \mathbf{A}_u \cdot \mathbf{X} = \sum_{v \in \mathcal{N}(u) \cap S} \frac{1}{\deg(u)} = \sum_{v \in \mathcal{N}(u) \cap S} p_{vu} \geq 1 - \prod_{v \in \mathcal{N}(u) \cap S} (1 - p_{vu}) = p(u|S). \tag{19}$$

- (16) can be proved by induction similar to Zhou et al. (2015). For every $p_v \leq 1$, the base case $\sum_{v \in \mathcal{X}} p_v p_{vu} \geq 1 - \prod_{v \in \mathcal{X}} (1 - p_v p_{vu})$ is obvious for $|\mathcal{X}| = 1$. For $|\mathcal{X}| > 1$, we have:

$$\begin{aligned}
1 - \prod_{v \in \mathcal{X}} (1 - p_v p_{vu}) &= 1 - (1 - p_x p_{xu}) \prod_{v \in \mathcal{X} \setminus x} (1 - p_v p_{vu})\\
&= 1 - \prod_{v \in \mathcal{X} \setminus x} (1 - p_v p_{vu}) + p_x p_{xu} \prod_{v \in \mathcal{X} \setminus x} (1 - p_v p_{vu})\\
&\leq \sum_{v \in \mathcal{X} \setminus x} p_v p_{vu} + p_x p_{xu} \prod_{v \in \mathcal{X} \setminus x} (1 - p_v p_{vu})\\
&\leq \sum_{v \in \mathcal{X} \setminus x} p_v p_{vu} + p_x p_{xu}\\
&= \sum_{v \in \mathcal{X}} p_v p_{vu}. && (20)
\end{aligned}$$

- (17), we have $p(u|v) = p_v p_{vu}$ per definition of the independent cascade, and consequently $p(u|S) = 1 - \prod_{v \in \mathcal{N}(u) \cap S} (1 - p_v p_{vu})$, where $p_v = 1$ for $v \in S^1$, which are the initial seed set that are activated deterministically. We can thus contend that Eq. equation 18 stands, and the computed probabilities are an upper bound of the real influence probabilities. Hence the influence spread, which is computed as $\hat{\sigma}(S) = \sum_{(u,v) \in E} p_{uv}$ is also an upper bound to the real $\sigma(S)$.

□

Now we address the theorem from Sec. 3.4 and detail the proof below.

Theorem 1. *The influence spread σ^m is submodular.*

For the purposes of the proof, $X_i \in \{0,1\}^{n\times d}$ is the input and $H_i \in \mathbb{R}^{n\times hd}$ is the output of the first neural layer for the input seed set S_i, and $P \in \{1\}^{hd\times 1}$. Moreover we define the support function $supp(v) = \{i \in [1,d], v_i \neq 0\}$ James et al. (2013) as the set of indices of non zero elements in vector $v \in \mathbb{R}^d$. Finally let R represent ReLU and b_{tr}, st_{tr} the mean and standard deviation computed by the batchnorm. Each step is justified further below.

Proof. $\forall i < j, S_i \subset S_j$:

$$supp(X_j) \supset supp(X(S_i)) \tag{21}$$
$$supp(X_jW) \supseteq supp(X(S_i)W) \tag{22}$$
$$supp(AX_jW) \supseteq supp(AX(S_i)W) \tag{23}$$
$$supp(R(AX_jW)) \supseteq supp(R(AX(S_i)W)) \tag{24}$$
$$supp\left(\frac{R(AX_jW) - b_{tr}}{st_{tr}}\right) \supseteq supp\left(\frac{(R(AX(S_i)W) - b_{tr})}{st_{tr}}\right) \tag{25}$$
$$supp(H_j) \supseteq supp(H(S_i)) \tag{26}$$
$$supp(H_jP) \supseteq supp(H(S_i)P) \tag{27}$$
$$|\mathbb{1}_{>0}\{H_jP\}| \geq |\mathbb{1}_{>0}\{H_iP\}| \tag{28}$$
$$|\mathbb{1}_{\leq 0}\{H_jP\}| \leq |\mathbb{1}_{\leq 0}\{H_iP\}| \tag{29}$$
$$A'_u\hat{L}_j \leq A'_u\hat{L}(S_i) \tag{30}$$
$$m_{S_j}[u] \leq m_{S_i}[u] \tag{31}$$
$$\sigma^m(S^j) + m_{S_j}[u] - \sigma^m(S^j) \leq \sigma^m(S^i) + m_{S_i}[u] - \sigma^m(S^i) \tag{32}$$
$$\sigma^m(S^j \cup \{u\}) - \sigma^m(S^j) \leq \sigma^m(S^i \cup \{u\}) - \sigma^m(S^i) \tag{33}$$
$$\tag{34}$$

1. (21) stems by the definition of X in Eq. (1).
2. (22) X_j is a convex hull that contains X_i Boyd et al. (2004). We multiply both sides by a real matrix $W \in \mathbb{R}^{d\times hd}$ which can equally dilate both convex hulls in terms of direction and norm. This equal transformation cannot change the sign of the difference between the elements of X_i and X_j and hence cannot interfere with the support of X_j over X_i. The statement becomes more obvious for $X \in \{0,1\}^{n\times 1}$ and $W \in \mathbb{R}^{1\times 1}$. Note that both can result in zero matrices so we use subset or equal.
3. (23) A is a non-negative matrix.
4. (24) ReLU is a non negative monotonically increasing function.
5. (25) Subtract by the same number and divide by the same positive number.
6. (26) Definition in Eq. (4).
7. (27) P is positive.
8. (28) By definition of the support.
9. (29) Complementarity between elements that are ≤ 0 and elements > 0.
10. (30) Definition in Eq. (10) and multiply with non-negative row u from matrix A'.
11. (31) Definition in Eq. (11).
12. (32) Adding and subtracting $\sigma^m(S^i)$ and $\sigma^m(S^j)$.
13. (33) By definition of σ^m in Eq. (12) we arrive at submodularity in Eq. (34).

□

APPENDIX B

B.1 GLIE TRAINING

We observed that $1,000$ has similar results to $10,000$, due to the small size of the networks. The training takes 500 up to $1,200$ seconds, depending on when the validation error converges. We have used a small scale grid-search to find the optimum batch size 64, dropout 0.4, number of layers 2, hidden layer size 64, and feature dimension 50. More importantly, we observed that it is beneficial to decrease the hidden layer size (by a factor of 2) as the depth increases, i.e., go from 32 to 16. This means that the 1-hop node representations are more useful compared to the 2-hop ones and so on—validating the aforementioned conclusion that the approximation to the influence estimation in Eq. (3), diverges more as the message passing depth progresses.

B.2 ADAPTIVE FULL FEEDBACK

We see here that the pattern that is prevalent in the two datasets described in section 3.4 is retained in other graphs.

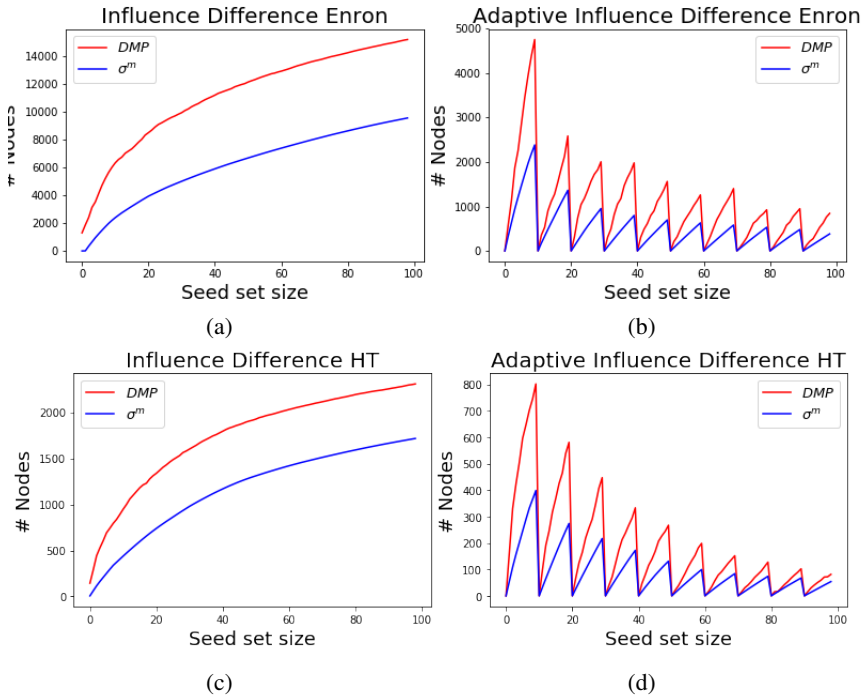

Figure 3: Difference between DMP influence estimate and σ^m in regular and adapting with full feedback every 10 seeds.

The results of PUN without AFF can be seen Tab. (6). The computational time is similar to the original PUN.

B.3 GLIE SUBMODULARITY AND MONOTONICITY

In this section we design an experiment to empirically prove that GLIE's output is submodular and monotonous. For each of the real datasets, we use the seed set retrieved by GLIE-CELF and a random seed set to quantify the differences between subsequent estimations. To be specific, we have a sequence S that represents the seed set and a sequence R that represents the random nodes, with

20 Seeds	100 Seeds
228	515
373	1,065
1305	2,303
8,200	14,920
4,227	8,369
103,846	189,547

Table 6: Influence spread results for PUN without AFF.

S_j being the seed set up to j^{th} element and s_j being the jth element, and similarly r_j for R. We compute the marginal gain to check for monotonicity:

$$m_{ss} = \hat{\sigma}(S_j \cup s_{j+1}) - \hat{\sigma}(S_j) \tag{35}$$

$$m_{sr} = \hat{\sigma}(S_j \cup r_{j+1}) - \hat{\sigma}(S_j), \tag{36}$$

and for submodularity, we have , with $i = j - 1$:

$$s_{ss} = (\hat{\sigma}(S_i \cup s_{j+1}) - \hat{\sigma}(S_i)) - (\hat{\sigma}(S_j \cup s_{j+1}) - \hat{\sigma}(S_j)) \tag{37}$$

$$s_{sr} = (\hat{\sigma}(S_i \cup r_{j+1}) - \hat{\sigma}(S_i)) - (\hat{\sigma}(S_j \cup r_{j+1}) - \hat{\sigma}(S_j)). \tag{38}$$

In Figures 4 to 7, we plot m and s for some of our datasets. Regarding s, since we require a constant node, we randomly sample one of the seeds s_j and a random node r_j and visualize the sequences of both s with regard to adding them in every step. The values of these functions correspond to nodes, and range from tens to thousands, depending on the datasets. For monotonicity and submodularity, we verify that m and s are always more than zero. Moreover, we see that they decrease with the size of the seed set, as well as the observation that adding a random seed provides worst marginal gains (in monotonicity plots) than adding the chosen seed.

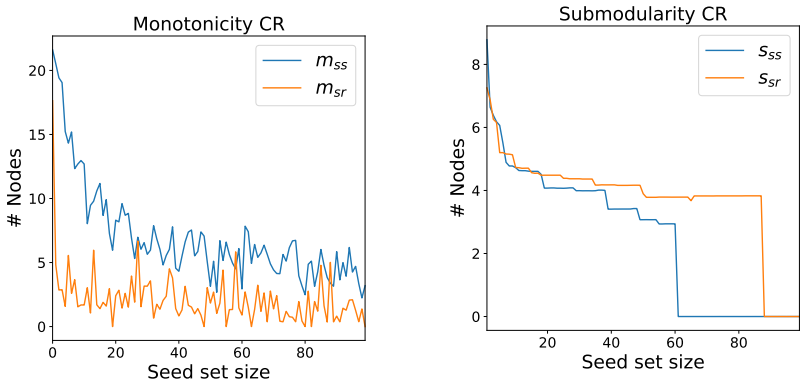

(a) (b)

Figure 4: Monotonocity and submodularity for the Crime (CR) dataset.

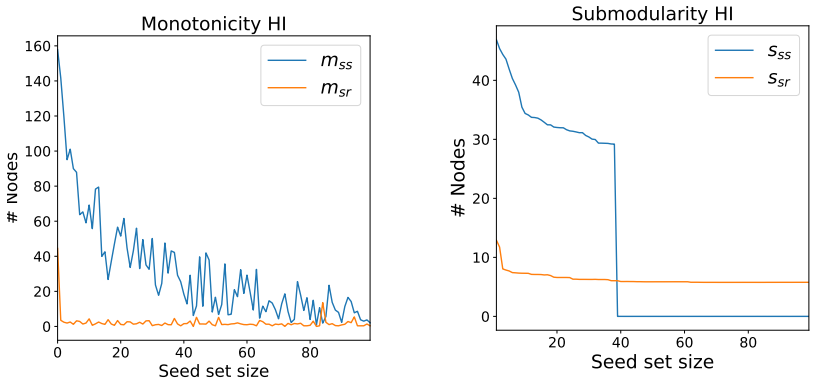

(a) (b)

Figure 5: Monotonocity and submodularity for the HI-II-14 (HI) dataset.

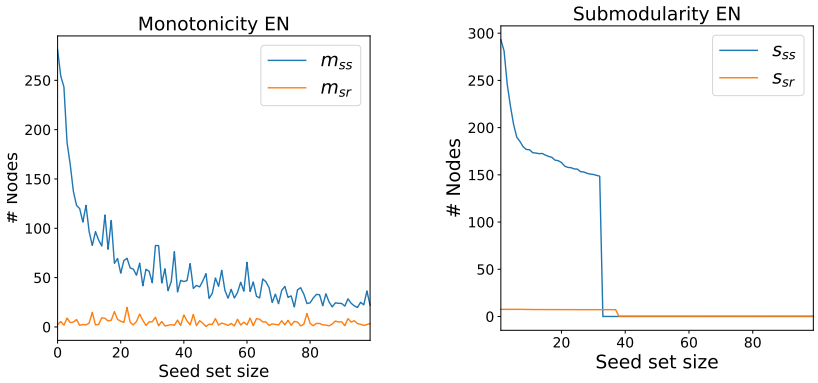

(a) (b)

Figure 6: Monotonocity and submodularity for the Enron (EN) dataset.

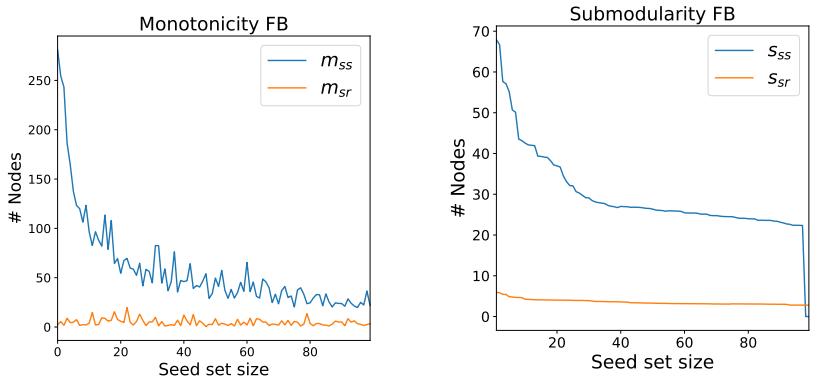

(a) (b)

Figure 7: Monotonocity and submodularity for the Facebook (FB) dataset.